https://doi.org/10.5194/gmd-2020-401
Preprint. Discussion started: 12 February 2021

Geoscientific Model Development Discussions

ShellChron 0.2.8: A new tool for constructing chronologies in accretionary carbonate archives from stable oxygen isotope profiles

Niels J. de Winter[1,2]

[1]Department of Earth Sciences, Utrecht University, Utrecht, the Netherlands

[2]AMGC research group, Vrije Universiteit Brussel, Brussels, Belgium

Corresponding author: Niels J de Winter (n.j.dewinter@uu.nl)

Abstract

This work presents ShellChron, a new model for generating accurate age-depth models for high-resolution paleoclimate archives, such as corals, mollusk shells and speleothems. Reliable sub-annual age models form the backbone of high-resolution paleoclimate studies. In absence of independent sub-annual growth markers in many of these archives, the most reliable method for determining the age of samples is through age modelling based on stable oxygen isotope or other seasonally controlled proxy records. ShellChron expands on previous solutions to the age model problem by modelling seasonal variability in the proxy record using a combination of growth rate and temperature sinusoids in sliding window approach. This new approach creates smoother, more precise age-depth relationships for multi-annual proxy records with the added benefit of allowing assessment of the uncertainty on the modelled age. The modular script of ShellChron allows the model to be tailored to specific archives, without being limited to $\delta^{18}O_c$ proxy records or carbonate archives, with high flexibility in assigning the relationship between the input proxy and the seasonal cycle. The performance of ShellChron in terms of accuracy and computation time is tested on a set of virtual seasonality records and real coral, bivalve and speleothem archives. The result shows that several key improvements in comparison to previous age model routines enhance the accuracy of ShellChron on multi-annual records while limiting its processing time. The current full working version of ShellChron enables the user to model the age of a 10-year long

https://doi.org/10.5194/gmd-2020-401
Preprint. Discussion started: 12 February 2021

Geoscientific Model Development Discussions

high-resolution (16 samples/yr) carbonate records with monthly accuracy within one hour of computation time on a modern personal computer. The model is freely accessible on the CRAN database and GitHub. Members of the community are invited to contribute by adapting the model code to suit their research topics.

1. Introduction

Fast growing carbonate archives, such as coral skeletons, mollusk shells and speleothems, contain a wealth of information about past and present climate and environment (e.g. Urban et al., 2000; Wang et al., 2001; Steuber et al., 2005; Butler et al., 2013). Recent advances in analytical techniques have improved our capability to extract this information and obtain records of the conditions under which these carbonates precipitated at high time resolutions, often beyond the annual scale (Treble et al., 2007; Saenger et al., 2017; Vansteenberge et al., 2019; de Winter et al., 2020a). Key to the interpretation of such records is the development of reliable chemical or physical proxies for climate and environmental conditions which can be measured on a sufficiently fine scale to allow variability to be reconstructed at the desired time resolution. Examples of suitable proxies include observations of variability in carbonate fabric and microstructure and in (trace) elemental and isotopic composition (Frisia et al., 2000; Lough, 2010; Ullmann et al., 2010; Schöne et al., 2011; Ullmann et al., 2013; Van Rampelbergh et al., 2014; de Winter et al., 2017). The unique preservation potential of carbonates in comparison with archives of climate variability at similar time resolutions, such as tree ring records and ice cores, now allows us to recover information about climate and environment of the geological past from these proxies on the (sub-)seasonal scale (Ivany and Runnegar, 2010; Ullmann and Korte, 2015; Vansteenberge et al., 2016; de Winter et al., 2018; 2020b; c; Mohr et al., 2020). The importance of this development cannot be overstated because variability at high (daily and seasonal) resolution constitutes the most significant component of climate variability (Mitchell, 1976; Huybers and Curry, 2006; Zhu et al., 2019). Accurate reconstructions of this type of variability are therefore fundamental to our understanding of Earth's climate system and critical for projecting of its behavior in the future under greenhouse warming conditions (IPCC, 2018).

https://doi.org/10.5194/gmd-2020-401
Preprint. Discussion started: 12 February 2021

A reliable age model is crucial to the interpretation of high-resolution carbonate records. An age model is defined as a set of rules or markers that allows the translation of the location of a measurement or observation on the archive to the time by which the carbonate was precipitated. This translation is required for aligning records from multiple proxies or archives to a common time axis. Age alignment enables data to be intercomparable and to be interpreted in the context of processes playing a role at similar timescales. Age models are based on knowledge about the growth or accretion rate of the archive through time. Many high-resolution carbonate archives contain growth markers on which age models can be based (e.g. Jones, 1983; Le Tissier et al., 1994; Verheyden et al., 2006). These are especially valuable in some mollusk species, in which growth lines demarcate annual, daily, or even tidal cycles (e.g. *Arctica islandica*, Schöne et al., 2005; *Pecten maximus*, Chavaud et al., 2005 and *Cerastoderma edule*, Mahé et al., 2010). However, in many mollusk species and most carbonate archives, such independent growth indicators are absent or too infrequent to (relatively) date high-resolution measurements (Judd et al., 2018; Huyghe et al., 2019). In such cases, age models need to be based on alternative indicators.

The oxygen isotope composition of carbonates ($\delta^{18}O_c$) is closely dependent on the isotopic composition of the fluid ($\delta^{18}O_w$) and the temperature by which the carbonate is precipitated (Urey, 1948; McCrea, 1950; Epstein et al., 1953). In most natural surface environments, either one or both factors is strongly dependent on the seasonal cycle, one being dominant over the other. This causes carbonates precipitated in these environments to display strong quasi-sinusoidal variations in $\delta^{18}O_c$ that follow the seasonal cycle (e.g. Dunbar and Wellington, 1981; Jones and Quitmyer, 1996; Baldini et al., 2008). Examples of this behavior include seasonal cyclicity in sea surface temperatures recorded in the $\delta^{18}O_c$ of corals and mollusks and seasonal cyclicity in the $\delta^{18}O_w$ of precipitation recorded in speleothems (Dunbar and Wellington, 1981; Schöne et al., 2005; Van Rampelbergh et al., 2014). These properties make $\delta^{18}O_c$ one of the most highly sought-after proxies for climate variability, and high-resolution $\delta^{18}O_c$ records are abundant in the paleoclimate literature (e.g. Lachniet, 2009; Lough, 2010; Schöne and Gillikin, 2013 and references therein).

The close relationship between $\delta^{18}O_c$ records and the seasonal cycle can also be exploited to estimate variability in growth rate of the archive. This property of $\delta^{18}O_c$ curves has been recognized by previous authors, and attempts have been made to quantify intra-annual growth rates from the shape of $\delta^{18}O_c$ profiles (Wilkinson and Ivany, 2002; Goodwin et al., 2003; De Ridder et al., 2006; Goodwin et al., 2009;

https://doi.org/10.5194/gmd-2020-401
Preprint. Discussion started: 12 February 2021

De Brauwere et al., 2009; Müller et al., 2015; Judd et al., 2018). Over time, these so called "growth models" have improved from fitting of sinusoids to $\delta^{18}O_c$ data (Wilkinson and Ivany, 2002; De Ridder et al., 2006) to including increasingly complicated (inter)annual growth rate curves to the model to fit the shape of the $\delta^{18}O_c$ data (Goodwin et al., 2003; 2009; Müller et al., 2015; Judd et al., 2018). These later models manage to fit the shape of $\delta^{18}O_c$ records well, but they often rely on detailed *a priori* knowledge of growth rate or temperature patterns (e.g. Goodwin et al., 2003; 2009), which causes them to rely on measurements of one or more parameters in the environment. These measurements are not available in studies on carbonate archives from the archeological or geological past. In contrast, the latest model by Judd et al. (2018) is based only on the assumption that growth and temperature follow quasi-sinusoidal patterns and can therefore work with $\delta^{18}O_c$ data alone, making it more widely applicable. The simplified parameterization of temperature and growth rate seasonality by Judd et al. (2018) using two (skewed) sinusoids is demonstrated to approximate natural circumstances very well.

However, the approach by Judd et al. (2018) is still limited in its use, because it requires whole, individual growth years to be analyzed separately, resulting in a discontinuous time series when applied on records containing multiple years of $\delta^{18}O_c$ data and no solution for incomplete years. In addition, the model has no option to supply information about the less dominant factor that drives $\delta^{18}O_c$ values ($\delta^{18}O_w$ of sea water in the case of mollusks and corals). Furthermore, only estimates from aragonite records are supported, while the other dominant carbonate mineral, calcite, has a different temperature relationship (Kim and O'Neil, 1997). Finally, neither of the models highlighted above except for the MoGroFun model by Goodwin et al. (2009) include any assessment of the uncertainty of the constructed age model.

Here, a new model for estimating ages of samples in seasonal $\delta^{18}O_c$ curves is presented which combines the advantages of previous models while attempting to negate their disadvantages. ShellChron combines a skewed growth rate sinusoid with a sinusoidal temperature curve to model $\delta^{18}O_c$ using the SCEUA optimization algorithm (Duan et al., 1992; following Judd et al., 2018). It applies this optimization using a sliding window through the dataset (as in Wilkinson and Ivany, 2002) and includes the option to use a Monte Carlo simulation approach to combine uncertainties on the input ($\delta^{18}O_c$ and depth measurements) and the model routine (as in Goodwin et al., 2009). As a result, ShellChron produces a continuous time series with a confidence envelope, supports records from multiple carbonate minerals and allows the user to provide information on the less dominant variable influencing $\delta^{18}O_c$ (e.g. $\delta^{18}O_w$) if available. The modular design of ShellChron's functional script allows parts of the model to be

https://doi.org/10.5194/gmd-2020-401
Preprint. Discussion started: 12 February 2021

Geoscientific Model Development Discussions

adapted and interchanged, supporting a wide range of climate and environmental archives. As a result, the initial design of ShellChron for reconstructing age models in temperature-dominated $\delta^{18}O_c$ records from marine bio-archives (e.g. corals and mollusks) presented here can be easily modified for application on other types of records. The routine is worked out into a ready-to-use package for the open-source computational programming language R and is directly available without restrictions, allowing all interested parties to freely modify and build on the base structure to adapt it to their needs (R Core Team, 2020; full package code and documentation in **SI1**, see also **Code availability**).

2. Stable oxygen isotope profiles in carbonate archives: The scientific basis

The relationship between $\delta^{18}O_c$ and the temperature of carbonate precipitation was first established by Urey (1951) and later refined with additional measurements and theoretical models (Epstein et al., 1953; Tarutani et al., 1969; Grossman and Ku, 1986; Kim and O'Neil, 1997; Coplen, 2007; Watkins et al., 2014; Daëron et al., 2019). Empirical transfer functions for aragonite and calcite by Grossmann and Ku (1986; modified by Dettmann et al., 1999; **equation 1**) and Kim and O'Neil (1997; **equation 2**, with VSMOW to VPDB scale conversion following Brand et al., 2014; **equation 3**) have so far found most frequent use in modern paleoclimate studies, and are therefore applied as default relationships in the ShellChron model (see *d18O_model* function).

$$T[°C] = 20.6 - 4.34 * (\delta^{18}O_c[‰VPDB] - \delta^{18}O_w[‰VSMOW] + 0.2) \quad (\mathbf{1})$$

$$1000 * \ln(\alpha) = 18.03 * \frac{10^3}{(T[°C] + 273.15)} - 32.42$$

$$with\ \alpha = \frac{\left(\frac{\delta^{18}O_c[‰VPDB]}{1000} + 1\right)}{\left(\frac{\delta^{18}O_w[‰VPDB]}{1000} + 1\right)} \quad (\mathbf{2})$$

$$\delta^{18}O_w[‰VPDB] = 0.97002 * \delta^{18}O_w[‰VSMOW] - 29.98 \quad (\mathbf{3})$$

To apply these formulae, it is assumed that carbonate is precipitated in equilibrium with the precipitation fluid. The question which carbonates are precipitated in equilibrium has long been subject to debate, and the development of new techniques for measuring the carbonate-water system (e.g. clumped and dual-clumped isotope analyses; Daëron et al., 2019; Bajnai et al., 2020) has led recent authors to

https://doi.org/10.5194/gmd-2020-401
Preprint. Discussion started: 12 February 2021

Geoscientific Model Development Discussions

challenge the assumption that equilibrium fractionation is the norm. These recent findings suggest that kinetic effects in fast-growing carbonate archives or elevated pH in the calcification fluids of some calcifiers (e.g. foraminifera and corals; Rollion-Bard et al., 2003; Zeebe, 2007) force precipitation out of equilibrium, and that true equilibrium is only reached in very slow-growing inorganic carbonates (e.g. Devils Hole vein calcite and subaqueous and cryogenic cave deposits; Coplen, 2007; Bajnai et al., 2020). On the other hand, disequilibrium fractionation likely affected the samples on which empirical transfer functions (**equations 1 and 2**) were based in a similar way as the samples on which they are applied, potentially eliminating the offset caused by disequilibrium fractionation (Daëron et al., 2019). In addition, the carbonic anhydrase enzyme present in many calcifiers accelerates CO_2 hydration at the calcification site, potentially eliminating kinetic effects in carbonate bio-archives whose growth rate would otherwise cause disequilibrium (Uchikawa and Zeebe, 2012). These findings are corroborated by many studies of modern marine calcifiers such as mollusks and corals in which $\delta^{18}O_c$-based temperatures closely match *in situ* water temperatures (Dunbar and Wellington, 1981; Jones and Quitmyer, 1996; Ullmann et al., 2010; de Winter et al., 2020c). Therefore, it is widely assumed that many marine calcifiers precipitate their carbonates near isotopic equilibrium and that the empirical transfer functions yield accurate temperature reconstructions. Note that the modular character of ShellChron allows the empirical transfer function to be adapted to the $\delta^{18}O_c$ record or to the user's preference for alternative transfer functions by a small modification of the *d18O_model* function, and that future versions of the model will include more options for changing the transfer function by default (see **Model description**).

As the name suggests, the ShellChron model was initially developed for application on $\delta^{18}O_c$ records from marine calcifiers (e.g. mollusk shells and corals). ShellChron approximates the temperature evolution at which the carbonate is precipitated by a sinusoidal function (see **equation 4** and **Table 1**; *temperature_curve* function; visualized in **Fig S1**), a good approximation of seasonal temperature fluctuations in most marine and terrestrial environments (Wilkinson and Ivany, 2002). Variability in $\delta^{18}O_w$ is also comparatively limited in most marine environments (except for regions with sea ice formation), making the model easy to use in these settings (LeGrande and Schmidt, 2006; Rohling, 2013). Nevertheless, ShellChron includes the option to provide *a priory* knowledge about $\delta^{18}O_w$, ranging from annual average values to detailed seasonal variability, enabling the model to work in environments with

https://doi.org/10.5194/gmd-2020-401
Preprint. Discussion started: 12 February 2021

Geoscientific Model Development Discussions

more complex interaction between $\delta^{18}O_w$ and temperature on the $\delta^{18}O_c$ record (see **equations 1 and 2**).

$$T[°C] = T_{av} + \frac{T_{amp}}{2} \sin\left(\frac{2\pi * \left(t[d] - T_{pha} + \frac{T_{per}}{4}\right)}{T_{per}}\right) \quad (4)$$

Table 1: Overview of model parameters

Name	Description	Unit	Range
T_{av}	Average temperature	°C	Variable, generally between 0°C–30°C
T_{amp}	Temperature range (2*amplitude)	°C	Variable, generally <20°C
T_{pha}	Phase of temperature sinusoid	d	0–365 days
T_{per}	Period of temperature sinusoid	d	365 days by default
G_{av}	Average growth rate	mm/d	Variable, generally between 0–100 mm/day
G_{amp}	Range of growth rates	mm/d	Variable, generally <200 mm/day
G_{pha}	Phase of growth rate sinusoid	d	0–365 days
G_{per}	Period of growth rate sinusoid	d	365 days by default
G_{skw}	Skewness factor of GR sinusoid	-	0–100, with 50 meaning no skew
D	Depth along the record	mm	Depends on archive
t	Age	d	Depends on archive
L_{win}	Length of sampling window	#	Depends on sampling resolution
w	Weighing factor on sample	-	0–1
i	Position relative to model window	-	0–L_i
I	Intercept of sinusoid (T_{av} or G_{av})		
A	Amplitude of sinusoid $\left(\frac{T_{amp}}{2}\ or\ \frac{G_{amp}}{2}\right)$		
P	Period of sinusoid (T_{per} or G_{per})	d	
φ	Phase of sinusoid (T_{pha} or G_{pha})	d	

If marine $\delta^{18}O_c$ records represent one extreme on the spectrum of temperature versus $\delta^{18}O_w$ influence on the $\delta^{18}O_c$ record, cave environments, in which $\delta^{18}O_c$ variability is predominantly driven by $\delta^{18}O_w$ variability in the precipitation fluid, represent the other extreme (Van Rampelbergh et al., 2014). In its current form, ShellChron takes $\delta^{18}O_w$ as a user-supplied parameter to model temperature and growth rate variability, but future versions will allow temperature to be fixed, while $\delta^{18}O_w$ becomes the modelled variable. ShellChron's modular character makes it possible to implement this update without changing the structure of the model. Application of ShellChron on $\delta^{18}O_c$ records from cave deposits will have to be treated with caution, since drip water $\delta^{18}O_w$ seasonality (if present) cannot always be approximated by a sinusoidal function and equilibrium fractionation in cave deposits is less common than in bio-archives (Baldini et al., 2008; Daëron et al., 2011; Van Rampelbergh et al., 2014).

https://doi.org/10.5194/gmd-2020-401
Preprint. Discussion started: 12 February 2021

Geoscientific Model Development Discussions
Open Access
EGU

Besides temperature (or $\delta^{18}O_w$) seasonality, ShellChron models the growth rate of the archive to approximate the $\delta^{18}O_c$ record (see **equation 5** and **Table 1**; *growth_rate_curve* function; visualized in **Fig S2**). Since the growth rate of many carbonate archives varies seasonally, a quasi-sinusoidal model for growth rate seems plausible (e.g. Le Tissier et al., 1994; Baldini et al., 2008; Judd et al., 2018). However, as discussed in Judd et al. (2018), the occurrence of growth cessations (growth rate = 0) and skewness in seasonal growth patterns calls for a more complex growth rate model that can take these properties into account. Therefore, ShellChron uses a slightly modified version of the skewed sinusoidal growth function described by Judd et al. (2018; **equation 5**). Note that the added complexity of this function does not preclude the modelling of growth rate functions described by a simple sinusoid (no skewness; G_{skw} = 50) or even constant growth through the year (G_{amp} = 0; see **Table 1**).

$$G[mm/yr] = G_{av} + \frac{G_{amp}}{2}\sin\left(\frac{2\pi * \left(t[d] - G_{pha} + G_{per} * S\right)}{P}\right)$$

$$with\ S = \begin{cases} \frac{100 - G_{skw}}{50}, & \text{if } t[d] - G_{pha} < G_{per}\frac{100 - G_{skw}}{100} \\ \frac{G_{skw}}{50}, & \text{if } t[d] - G_{pha} \geq G_{per}\frac{100 - G_{skw}}{100} \end{cases} \quad (5)$$

Contrary to previous $\delta^{18}O_c$ growth models, ShellChron allows uncertainties on the input variables (depth and $\delta^{18}O_c$ measurements) as well as uncertainties of the full modelling approach to be propagated, providing confidence envelopes around the chronology. Uncertainty propagation is optional and can be skipped without compromising model accuracy. Standard deviations of uncertainties on input variables (depth and $\delta^{18}O_c$) can be provided by the user, while model uncertainties are calculated from the variability in model results of the same datapoint obtained from overlapping simulation windows (see *growth_model* function). Measurement errors are combined by projecting Monte Carlo simulated values for depth and $\delta^{18}O_c$ measurements on the modelled $\delta^{18}O_c$ curve through an orthogonal projection (**equation 6**; *mc_err_orth* function; visualized in **Fig S3**). The measurement uncertainty projected on the depth domain is then combined with the model uncertainty to obtain pooled uncertainties in the depth domain, which are propagated through the modelled $\delta^{18}O_c$ record to obtain uncertainties on the model result in the age domain. As a result of the sliding window approach in ShellChron, model results for datapoints situated at the edges of windows are more sensitive to small changes in the modelled parameters and therefore possess a larger model uncertainty. To prevent these less certain model estimates from affecting the stability of the model, model results were given more weight the closer they

https://doi.org/10.5194/gmd-2020-401
Preprint. Discussion started: 12 February 2021

Geoscientific Model Development Discussions

were situated towards the center of the model window (see **equation 7** in *export_results* function; see also **Fig. S4**). This weighing is also incorporated in uncertainty propagation through a weighted standard deviation (see **equation 8** from the *sd_wt* function).

$$\sigma_{meas} = \sqrt{\left(\frac{D_{sim} - \overline{D_{sim}}}{\sigma_D}\right)^2 + \left(\frac{\delta^{18}O_{sim} - \overline{\delta^{18}O_{sim}}}{\sigma_{\delta^{18}O}}\right)^2} \quad (6)$$

$$w[i] = 1 - \left|\frac{2i}{L_{window}} - 1\right| \quad (7)$$

$$\sigma_{weighted,i} = \sqrt{\frac{w_i * (x_i - \bar{w})^2}{\sum w[i] * \frac{N-1}{N}}} \quad (8)$$

3. Model description

ShellChron is organized in a series of functions that describe the step-by-step modelling process. A schematic overview of the model is given in **Fig. 1**. A wrapper function (*wrap_function*) is included which carries out all steps of the model procedure in succession to promote ease of use.

https://doi.org/10.5194/gmd-2020-401
Preprint. Discussion started: 12 February 2021

Geoscientific Model Development Discussions
Open Access
EGU

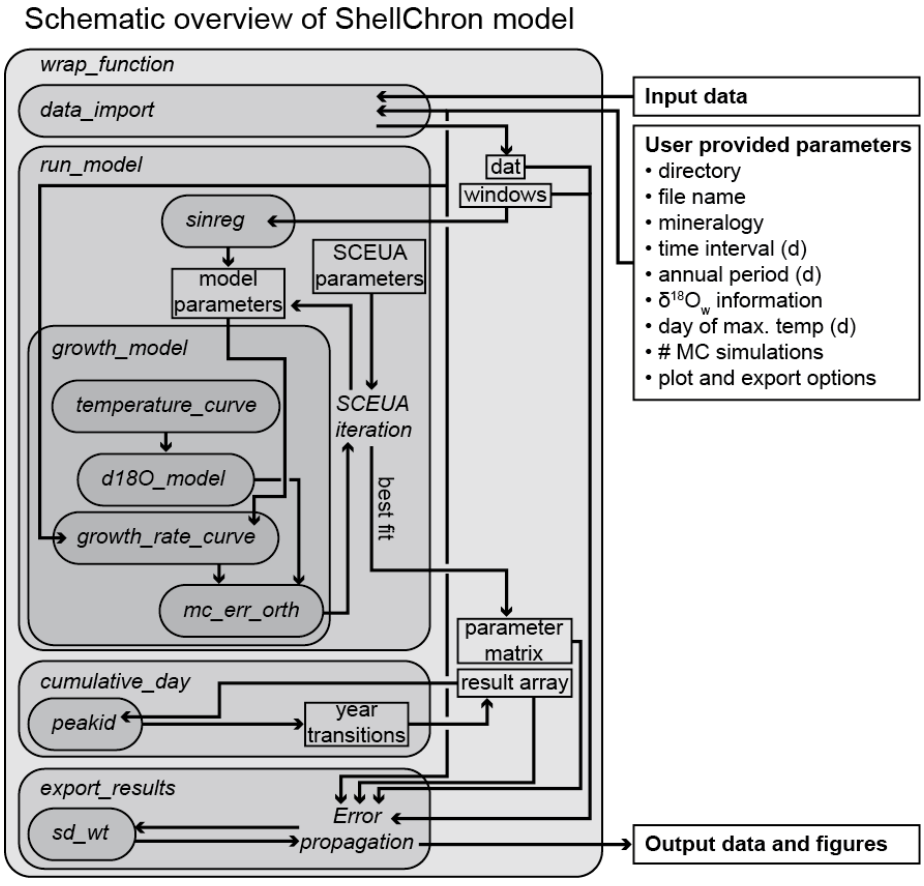

Figure 1: Schematic overview of ShellChron. Names in *italics* refer to functions (encapsulated in rounded rectangular boxes) and operations within functions. Rectangular boxes represent data. Arrows represent the flow of information between model components. Note that some operations are encapsulated in functions (e.g. *Error propagation* in *export results*) and that some functions are only used within other functions (e.g. *peakid* in *cumulative_day*). All data structures outside *wrap_function* represent input and output of the model. Detailed documentation of all functions and operations in ShellChron is provided in **SI1**.

https://doi.org/10.5194/gmd-2020-401
Preprint. Discussion started: 12 February 2021

Data is imported through the *data_import* function, which takes a comma-separated text file (CSV) with the input data. Data files need to contain columns containing depth (*D*) and $\delta^{18}O_c$ data, a column marking years in the record and two optional columns containing uncertainties on depth ($\sigma(D)$, one standard deviation) and $\delta^{18}O_c$ ($\sigma(\delta^{18}O_c)$, one standard deviation) respectively (see example in **SI2** and **Figure 2**). The function uses the year markers (third column) as guidelines for defining the minimum length of the model windows to ensure that all windows contain at least one year of growth. Consecutive windows are shifted by one datapoint, yielding a total number of windows equal to the sample size minus the length of the last window. The result of the model does not otherwise depend on user-provided year markers, instead basing the age result purely on simulations of the $\delta^{18}O_c$ data.

https://doi.org/10.5194/gmd-2020-401
Preprint. Discussion started: 12 February 2021

Geoscientific Model Development
Discussions
Open Access
EGU

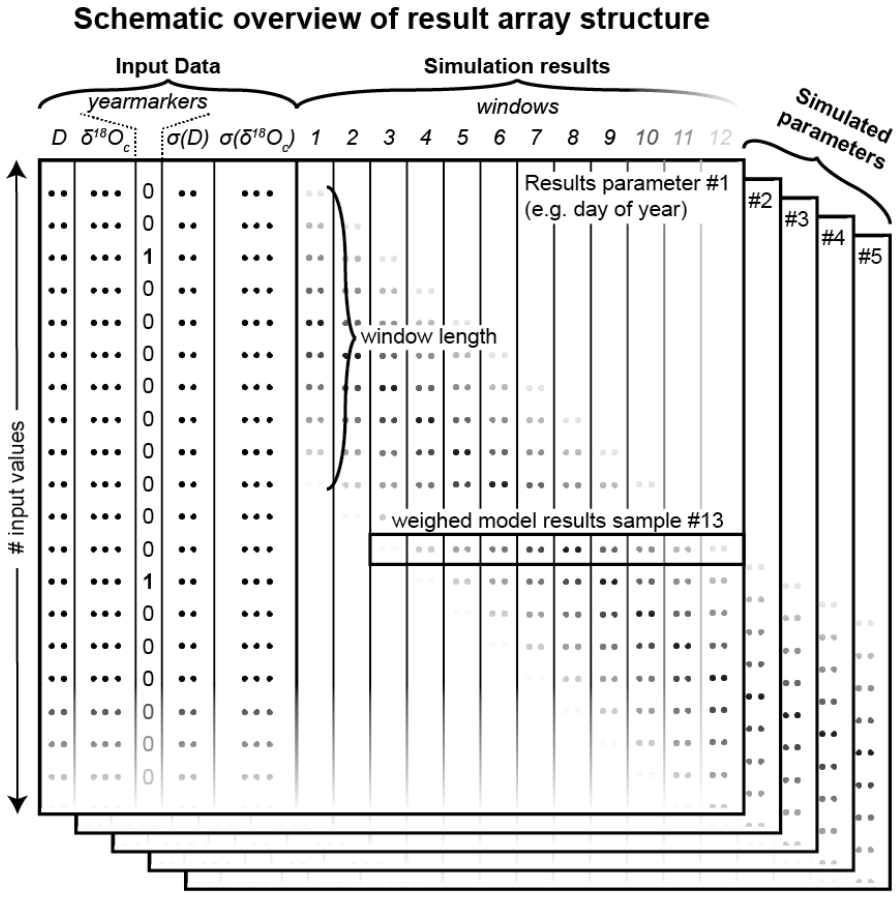

243

244 **Figure 2:** Schematic overview of the structure of the result array in which ShellChron stores the raw
245 results of each model window. Data is stored in three dimensions: The sample number (rows in the
246 figure), the window number (columns in the figure) and the number of modelled parameters (represented
247 by the stacked table “sheets” in the figure). Note that the first 5 columns of each “sheet” represent the
248 user-provided input data (see example in **SI2**), and that the model result data starts from column 6. The
249 window length is determined by the user-provided indication of year transitions (column 3). Rows of dots
250 in the figure are placeholders for (input or result) values. Shading of these dots in the window columns
251 indicate differential weighing of modelled values in function of their location relative to the sliding window.
252 The horizontal box shows how these weighing factors within each sample window (in vertical direction)
253 result in weighing of different estimates of modelled parameters for the same data point (in horizontal
254 direction). Shading of input data and window number towards the bottom and right edge of the figure,

https://doi.org/10.5194/gmd-2020-401
Preprint. Discussion started: 12 February 2021

Geoscientific Model Development Discussions

255 respectively, indicates that the number of input values (and thus simulation windows) is only limited to
256 the length of the input table and may therefore continue indefinitely (at the expense of longer
257 computation times, see **Figure 5** in **Model performance**).

258

https://doi.org/10.5194/gmd-2020-401
Preprint. Discussion started: 12 February 2021

Geoscientific Model Development Discussions

The core of the model consists of simulations of overlapping subsamples (windows) of the depth and $\delta^{18}O_c$ data described by the *run_model* function (see **Fig. 1 and 2**). Data and window sizes are passed from *data_import* onto *run_model* along with user-provided parameters (e.g. $\delta^{18}O_w$ information; see **Fig. 1**). *run_model* loops through the data windows and calls the *growth_model* function, which fits a modelled $\delta^{18}O_c$ vs. depth curve through the data using the SCEUA optimization algorithm (see Duan et al., 1992). The simulated $\delta^{18}O_c$ curve is produced through a combination of a temperature sinusoid (*temperature_curve* function; see **equation 4** and **Fig. S1**) and a skewed growth rate sinusoid (*growth_rate_curve*; see **equation 5** and **Fig. S2**), with temperature data converted to $\delta^{18}O_c$ data through the *d18O_model* function (**equation 1 and 2**). Starting values for the parameters describing temperature and growth rate curves are obtained by estimating the annual period (*P*) through a spectral density estimation and applying a linearized sinusoidal regression through the $\delta^{18}O_c$ data (*sinreg* function; see **equation 9**). In addition, *growth_model* takes a series of fixed parameters describing the method for SCEUA optimization (see Duan et al., 1992; Judd et al., 2018) and the upper and lower bounds for parameters describing temperature and growth rate curves (see **SI3**). If uncertainties on depth and $\delta^{18}O_c$ data are provided, *growth_model* calls the *mc_err_orth* function to propagate these errors through the model result (see **equation 6** and **Fig S3**).

$$\delta^{18}O_c[‰VPDB] = I + \frac{A}{2}\sin\left(\frac{2\pi * \left(D - \varphi + \frac{P}{4}\right)}{P}\right),$$

$$linearized\ as{:}\ \delta^{18}O_c[‰VPDB] = a + b\sin\left(\frac{2\pi}{P} * D\right) + c\cos\left(\frac{2\pi}{P} * D\right),$$

$$with\ I = a; A = \sqrt{b^2 + c^2}\ and\ \varphi = P * \left(0.25 - \frac{\cos^{-1}\left(\frac{b}{A}\right)}{2\pi}\right) \quad (9)$$

The *run_model* function returns an array listing day of the year (1–365), temperature, $\delta^{18}O_c$, growth rate and (optionally) their uncertainty standard deviations as propagated from uncertainties on the input data ("result array"; see **Fig. 2** and **SI4**). In addition, a matrix containing the optimized parameters of temperature and growth rate curves is provided, yielding information about the evolution of mean values, phases, amplitudes, and skewness of seasonality in temperature and growth rate along the record ("parameter matrix", see **Fig. 1** and **SI5**). To construct an age model for the entire record, the modelled timing of growth data, expressed as day relative to the 365-day year, needs to be converted into a

https://doi.org/10.5194/gmd-2020-401
Preprint. Discussion started: 12 February 2021

Geoscientific Model Development Discussions

cumulative time series listing the number of days relative to the start of the first year represented in the record (rather than relative to the start of the year in which the datapoint is found). This requires year transitions (transitions from day 365 to day 1) to be recognized in all the model results. The *cumulative_day* function achieves this by aggregating information about places where the beginning and end of the year is recorded in individual window simulations and applying a peak identification algorithm (*peakid* function) to find places in the record where year transitions occur (see **Supplementary Methods**). Results of the timing of growth for each sample (in day of the year) are converted to a cumulative time scale using their positions relative to these recognized year transitions (**Supplementary Methods**).

In a final step (described by the *export_results* function), the results from overlapping individual modelling windows are combined to obtain mean values and confidence envelopes of the result variables (age, $\delta^{18}O_c$, $\delta^{18}O_c$-based temperatures and growth rates) for each sample in the input data. If uncertainties on the input variables were provided, these are combined with uncertainties on the modelling result calculated from results of the same datapoint on overlapping data windows by pooling the variance of the uncertainties (**equation 10**). Throughout this merging of data from overlapping windows, results from datapoints on the edge of windows are given less weight than those from datapoints near the center of a window (see **equation 7** and **Fig. S4**). This weighing procedure corrects for the fact that datapoints near the edge of a window are more susceptible to small changes in the model parameters and are therefore less reliable than results in the center of the window. Finally, summaries of the simulation results and the model parameters including their confidence intervals are exported as comma-separated (CSV) files. In addition, *export_results* supports optional exports of figures displaying the model results and files containing raw data of all individual model windows (equivalent to “sheets” of the result array, see **Fig. 2** and **SI4**).

$$VAR_{pooled} = \frac{\sum_i((N_i - 1) * VAR_i * w_i)}{\sum_i(N_i) - n} \quad (10)$$

in which w = weight of the individual reconstructions, N is the sample size and n is the number of reconstructions (indexed by i) that is combined

https://doi.org/10.5194/gmd-2020-401
Preprint. Discussion started: 12 February 2021

Geoscientific Model Development Discussions

4. Model performance

The performance of ShellChron was tested on two virtual datasets: a $\delta^{18}O_c$ record constructed from a simulated temperature sinusoid with added stochastic noise (**Case 1**; **SI6**) and one based on a real high-resolution sea surface temperature and salinity record measured on the coast of Texel island in the tidal basin of the Wadden Sea in the north of the Netherlands (**Texel**, see details in **SI7** and de Winter et al., 2020d and **Supplementary Methods**). In addition, three modern carbonate $\delta^{18}O_c$ records were internally dated using ShellChron: a tropical stony coral (*Porites lutea*; hereafter: **coral**) from the Pandora Reef (Great barrier Reef, NE Australia; Gagan et al., 1993; see **SI8**), a Pacific oyster shell (*Crassostrea gigas*; hereafter: **oyster**) from List Basin in Denmark (Ullmann et al., 2010; see **SI8**) and a temperate zone speleothem from Han-sur-Lesse cave (Belgium; hereafter: **speleothem**; see Vansteenberge et al., 2019; see **SI8**). Finally, ShellChron's performance in terms of computation time and accuracy is compared to that of the most comprehensive pre-existing $\delta^{18}O_c$-based age model (by Judd et all., 2018) on simulated temperature sinusoids of various length and sampling resolutions to which stochastic noise was added (*sensu* **Case 1**; de Winter et al., 2020d; see **SI9**). The latter also demonstrates the scalability of ShellChron and its application on a variety of datasets. Timing comparisons were carried out using a modern laptop (Dell XPS13–7390; Dell Inc., Round Rock, Tx, USA) with an Intel Core i7 processor (8 MB cache, 4.1 GHz clock speed, 4 cores, Intel Corporation, Santa Clara, CA, USA), 16 GB LPDDR3 RAM and a SSD drive running Windows 10. Note that ShellChron was built and tested successfully on Mac OS, Fedora Linux and Ubuntu Linux as well.

https://doi.org/10.5194/gmd-2020-401
Preprint. Discussion started: 12 February 2021

Geoscientific Model Development Discussions

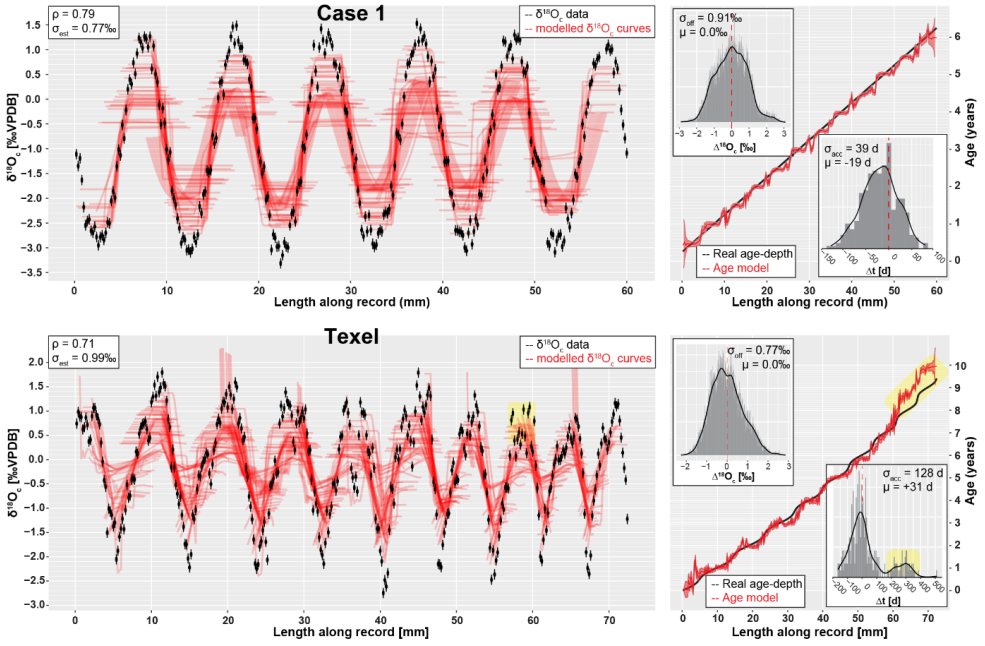

Figure 3: Result of applying ShellChron on the two virtual datasets: **Case 1** (top, see **SI6**) and **Texel**, (bottom, see **SI7**). Leftmost panels show the model fit of individual sample windows (red) on the data (black, including horizontal and vertical error bars), with in the top left Spearman's correlation coefficients (ρ) and standard deviations on the $\delta^{18}O_c$ estimate (σ_{est}). Right panels show the resulting age model (red, including shaded 95% confidence level) compared with the real age-depth relationship of both records. Histograms in the top left of age-depth plots show the offset between modelled and measured $\delta^{18}O_c$ (as visualized in the left panel) with standard deviations of the $\delta^{18}O_c$ offset (σ_{off}) and offset averages (μ). Histograms in the bottom right of age-depth plots show the offset between modelled and actual ages (in days) of each datapoint, including standard deviations on the age accuracy (σ_{acc}) and mean age offset (μ). Note that the last 2 years' worth of data in the **Texel** dataset (shaded in yellow) show a positive offset of almost 1 year due to an aberration in the data around 60 mm (see discussion in text).

https://doi.org/10.5194/gmd-2020-401
Preprint. Discussion started: 12 February 2021

Geoscientific Model Development Discussions
Open Access
EGU

345 Results of running ShellChron on **Case 1** and **Texel** datasets (**Fig. 3**) show that modelled $\delta^{18}O_c$ records
346 in individual windows closely match the data. A summary of ShellChron performance statistics is given
347 in **Table 2**. In both virtual datasets, $\delta^{18}O_c$ estimates are equally distributed above and below the $\delta^{18}O_c$
348 data ($\overline{\Delta^{18}O_c} = 0.0$ ‰; Spearman's ρ of 0.79 and 0.71 for **Case 1** and **Texel** datasets respectively) and
349 show no seasonal bias (see **SI10**) in both datasets. The fact that this is also the case for the **Texel**
350 dataset, which is skewed towards growth in the winter season and includes relatively strong seasonal
351 variability in $\delta^{18}O_w$, shows that ShellChron is not sensitive to such subtle (though common) variability in
352 growth rate or $\delta^{18}O_w$. In general, ShellChron's mean age assignment is accurate on a monthly scale
353 (age offsets of -19 ± 39 d and +31 ± 128 d for **Case 1** and **Texel** datasets respectively). The **Texel** data
354 contains some notable exceptions near the end of the record, where the sampling resolution is reduced
355 (see **SI7**) resulting in an overestimation of the age for data in the last two years in the record. On closer
356 inspection, the inaccuracies result from a persistent reduction of $\delta^{18}O_c$ in the winter season around 60
357 mm along the record which is interpreted by the model as an extra annual cycle. This glitch results from
358 the interplay of seasonally low $\delta^{18}O_w$ values and stochastic noise in high-resolution records and warrants
359 *a posteriori* inspection of model results by the user. The offset in the last part of the record can be easily
360 spotted by inspecting the growth curve and amended by subtracting the extra year from the affected
361 datapoints. After correction, the accuracy of modelling the **Texel** age becomes (-22 ± 80 d).

362

https://doi.org/10.5194/gmd-2020-401
Preprint. Discussion started: 12 February 2021

Geoscientific Model Development Discussions
Open Access
EGU

Table 2: Overview of datasets and model results

Dataset	Resolution	Length	$\delta^{18}O_c$ seasonal range	Complications
Case 1	50 yr^{-1}	6 yr	~4.3‰	None
Texel	26–45 yr^{-1}	10 yr	~4‰	Variable $\delta^{18}O_w$, Variable GR
Coral	30–49 yr^{-1}	6 yr	~1.7‰	Variable GR
Oyster	23–45 yr^{-1}	3.5 yr	~3‰	Variable $\delta^{18}O_w$, Variable GR
Speleothem	4–13 yr^{-1}	14 yr	~0.5‰	Variable $\delta^{18}O_w$, Variable GR, Non-sinusoidal $\delta^{18}O_c$-forcing

Dataset	$\delta^{18}O_c$ offset	Age offset	Spearman's ρ	Observations
Case 1	0.0 ± 0.91‰	-19 ± 39 d	0.79	-
Texel	0.0 ± 0.77‰	+31 ± 128 d (-21 ± 80 d)	0.71	Last 2 years off
Coral	0.0 ± 0.15‰	-22 ± 44 d	0.96	-
Oyster	0.0 ± 0.35‰	-9 ± 53 d	0.91	Reduced accuracy near growth stops
Speleothem	0.0 ± 0.13‰	105 ± 166 d	0.71	Only reliable on inter-annual scale

363

https://doi.org/10.5194/gmd-2020-401
Preprint. Discussion started: 12 February 2021

Geoscientific Model Development
Discussions
Open Access
EGU

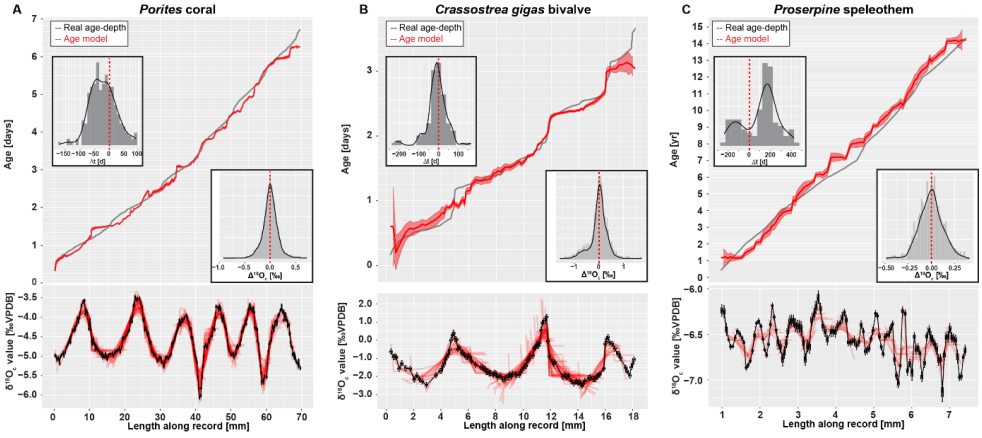

Figure 4: Overview of model results for the three test datasets from real carbonate archives: (**A**) **coral**, (**B**) **oyster** and (**C**) **speleothem**. Lower panels indicate the fit of individual model windows (in red) with the data (in black) while upper panels show the age model (in red) compared to the "true" age-depth relationship with histograms showing model accuracy (in days, top left) and model fit ($\delta^{18}O_c$ offset in ‰, bottom right). Color scheme follows **Figure 3**. Note that the true age-depth relationship is not known for these natural records, but is estimated using known growth seasonality (**coral**), comparison with *in situ* temperature and salinity measurements (**oyster)** or simply by interpolating between annual growth lines (**speleothem**). See **Supplementary Methods** for details.

https://doi.org/10.5194/gmd-2020-401
Preprint. Discussion started: 12 February 2021

Geoscientific Model Development Discussions

Results of modelling natural carbonate records (**Fig. 4** and **Table 2**) illustrate the effectiveness of ShellChron on different types of records. Performance clearly depends on the resolution of the record and the regularity of seasonal variability contained within. As in the virtual datasets, modelled $\delta^{18}O_c$ successfully mimic $\delta^{18}O_c$ data in all records ($\overline{\Delta^{18}O_c} = 0.0$; Spearman's ρ of 0.96, 0.91 and 0.71 for **coral**, **oyster** and **speleothem** respectively). No consistent seasonal bias is observed in $\Delta^{18}O_c$ and model accuracy ($p>0.05$; see **Table 2** and **SI10**), despite significant (seasonal and inter-annual) variability contained in the records (especially in **oyster** and **speleothem** records). When comparing the accuracy of these records, it must be noted that the "real" age of the samples in these natural carbonates is not known with accuracy. Model results are instead compared with age models constructed using conventional techniques such as matching $\delta^{18}O_c$ profiles with local temperature and/or $\delta^{18}O_w$ variability (**oyster** and **coral** records) or even merely by linear interpolation between annual markers in the record (**speleothem** record; see **Supplementary Methods**). Despite this caveat, testing results clearly show that the least complicated record (**coral**; **Fig. 4a**), characterized by minimal variability in $\delta^{18}O_w$ and growth rate and a high sampling density, has the best overall model result ($\Delta^{18}O_c = 0.0 \pm 0.15$ compared to a ~1.7‰ seasonal range; $\rho = 0.96$; $\Delta t = -22 \pm 44$ d; see **Table 2**). The **oyster** record (**Fig. 4b**), which has strong seasonal variability in growth rate and $\delta^{18}O_{sw}$ also yields a very reliable age model ($\Delta^{18}O_c = 0.0 \pm 0.15$ compared to a ~3‰ seasonal range; $\rho = 0.91$; $\Delta t = -9 \pm 53$ d; see **Table 2**). The **speleothem** record (**Fig. 4c**), plagued by lower sampling resolution, large inter-annual $\delta^{18}O_c$ variability, restricted $\delta^{18}O_c$ seasonality and a lack of clearly seasonal $\delta^{18}O_c$ forcing, yields the least reliable model result ($\Delta^{18}O_c = 0.0 \pm 0.13$ compared to a ~0.5‰ seasonal range; $\rho = 0.71$; $\Delta t = 105 \pm 166$ d; see **Table 2**). Note that the accuracy figure provided for the **speleothem** record is based on comparison with an age model based on linear interpolation between annual growth lines. Since no reliable information is available on sub-annual variability in growth rates in this record, ShellChron results cannot be validated at the sub-annual scale in this case.

https://doi.org/10.5194/gmd-2020-401
Preprint. Discussion started: 12 February 2021

Geoscientific Model Development Discussions
Open Access
EGU

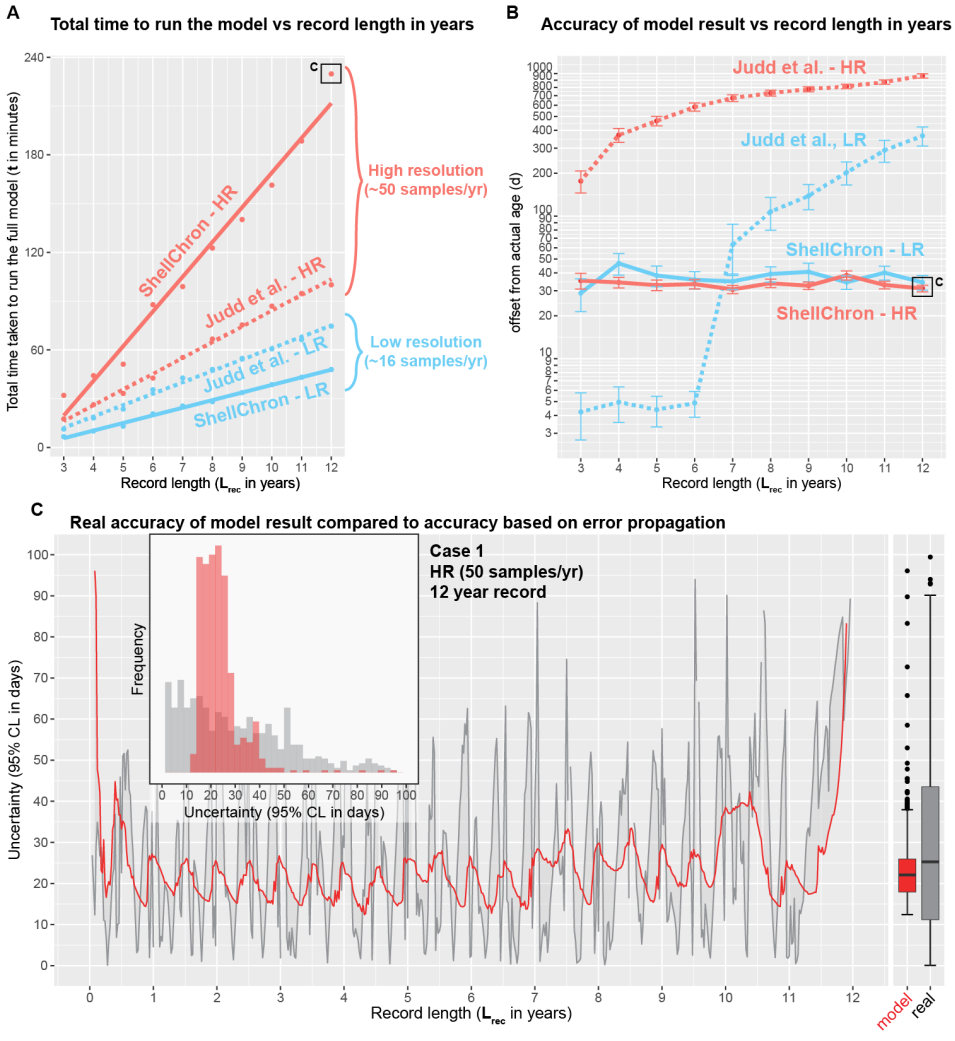

Figure 5: Overview of the result of timing ShellChron and the Judd et al. (2018) model on the same datasets (**A**), comparing the accuracies of both models (**B**) and comparing the accuracy as calculated by ShellChron with the real offset in the age model (**C**). In (**A**) and (**B**), low resolution datasets are plotted in blue, while high-resolution datasets plot in red. Solid lines represent ShellChron and dashed lines show performance of the Judd et al. model. The black box in (**A**) and (**B**) highlights the dataset used in (**C**). In (**C**), grey lines, bars and boxplot indicate true offset of the model from the actual sample age, while red lines, bars and boxplot show the accuracy of the model as calculated from the propagated errors on model and input data.

https://doi.org/10.5194/gmd-2020-401
Preprint. Discussion started: 12 February 2021

The performance of both ShellChron and the Judd et al. model in terms of computation time linearly increases with the length of the record (in years; see **Fig. 5**, **Fig. S5** and **SI9**). Computation time of ShellChron on the high-resolution test dataset (50 samples/yr) increases very steeply with the length of the record in years (~21 minutes per additional year), while the low-resolution dataset (16 samples/yr) shows a slower increase (~5 minutes per additional year; **Fig. 5A**). This contrasts with the model from Judd et al., which requires only slightly more time on high-resolution data than on low-resolution datasets (~7 and ~10 minutes per additional year, respectively). The difference is explained by the sliding window approach applied in ShellChron, which requires more SCEUA optimization runs per year in high-resolution datasets than in low resolution datasets. When plotted against the number of calculation windows or samples in the dataset, running ShellChron on low-resolution and high-resolution datasets require a similar increase in computation time (~0.4 minutes, or 24 seconds, per additional sample/window; **Fig. S5**). ShellChron thus outcompetes the Judd et al. model in terms of computation time in datasets with fewer than ~20 samples per year, even though more SCEUA optimizations are required.

The key computational improvement in ShellChron is the application of a sinusoidal regression before each SCEUA optimization to estimate the initial values of the modelled parameters (*sinreg* function; see **equation 9** and **Fig. 1** in **Model description**). Since carbonate archives are rarely sampled for stable isotope measurements above 20 samples per year (e.g. Goodwin et al., 2003; Schöne et al., 2005; Lough, 2010 and references therein), the disadvantage of a steep computational increase for very high-resolution archives is, in practice, a favorable tradeoff for the added control on model and measurement uncertainty and smoother inter-year transitions ShellChron offers in comparison to previous models. The similarity of ShellChron's accuracy in the low- and high-resolution datasets demonstrates its robustness across datasets with various sampling resolutions (see also **Table 2** and **Fig. 4B**).

Longer computation times in the Judd et al. model result in better accuracy on the modelled age compared to the present version of ShellChron on the scale of individual datapoints (see **Fig. 5**). However, this advantage is rapidly lost when records containing multiple years are considered (**Fig. 5B**). The advantage of the ShellChron model is its application of overlapping model windows, which smooth out the transitions between modelled years and eliminate accumulations of model inaccuracies when records grow longer. In addition, contrary to previous models, ShellChron does not rely on user-defined year boundaries, which may introduce mismatches between subsequent years to be propagated

https://doi.org/10.5194/gmd-2020-401
Preprint. Discussion started: 12 February 2021


Geoscientific Model Development Discussions

through the age model, even in ideal datasets such as **Case 1** (**Fig. 5B**; see also **Supplementary Methods**). By comparison, the overall accuracy of ShellChron is much more stable within and between datasets of different length, while rarely introducing offsets of more than a month. More importantly, where ShellChron takes into account the uncertainty on input parameters, this uncertainty is not considered in most previous models (the MoGroFun model of Goodwin et al., 2003 being the exception). The added uncertainty caused by input error is higher in less regular (sinusoidal) $\delta^{18}O_c$ records and in records with lower sampling resolution, causing the uncertainties on the Judd et al., model reported here for the ideal, high-resolution **Case 1** dataset to be over-optimistic. If ShellChron's model accuracy is insufficient, its modular character allows the user to run the SCEUA algorithm to within more precise optimization criteria by changing the model parameters (see **SI3**). However, this adaptation comes at a cost of longer computation times.

The estimated uncertainty envelope (95% confidence interval) on the modelled age calculated by the error propagation algorithm in ShellChron (24 ± 14 d) on average slightly underestimates the actual offset between modelled age and real age in the **Case 1** record (31 ± 24 d; $p_{difference} < 0.05$; **Fig. 5C**). The foremost difference between modelled and real uncertainty on the result is that the modelled uncertainty yields a more smoothed record of uncertainty compared to the record of actual offset of the model (**Fig. 5C**). ShellChron's uncertainty calculations are partly based on comparing overlapping model windows, thereby smoothing out short term variations in model offset. The uncertainty of the model result (both real and modelled) shows regular variability with a period of half a year (**Fig. 5C**). Comparing this variability with the phase of the record (of which 6 years are plotted in **Fig. 3A**) reveals that the uncertainty of the model is positively correlated to the slope of the $\delta^{18}O_c$ record. This is expected, because in parts of the record with steep $\delta^{18}O_c$-depth slopes, the local age model result is more sensitive to small changes in the depth domain, caused either by uncertainty in the model fit or propagated uncertainty on the depth value defined by the user.

5. Applications and discussion

Its new features compared to previous age model routines make ShellChron a versatile package for creating age models in a range of high-resolution paleoclimate records. The discussion above demonstrates that ShellChron can reconstruct the age of individual $\delta^{18}O_c$ samples within monthly

https://doi.org/10.5194/gmd-2020-401
Preprint. Discussion started: 12 February 2021


Geoscientific Model Development Discussions

precision. This level of precision is sufficient for accurate reconstructions of seasonality, defined as the difference between warmest and coldest month (following USGS definitions; O'Donnell and Ignizio, 2012). While an improvement on this uncertainty could be of potential interest for ultra-high-resolution paleoclimate studies (e.g. sub-daily variability, see Sano et al., 2012; Yan et al., 2020; de Winter et al., 2020a), the increase in computation time and the sampling resolution such detailed age models demand render age modelling from $\delta^{18}O_c$ records inefficient for this purpose. The sampling resolution for high-resolution carbonate $\delta^{18}O_c$ records in the literature does not typically exceed 0.1 mm due to limitations in sampling acquisition (e.g. micromilling), which even in fast-growing archives limits the resolution of these records to several days at best (see Gagan et al., 1994; Van Rampelbergh et al., 2014; de Winter et al., 2020c). While in some archives, high-resolution (< 100 µm) trace element records could be used to capture variability beyond this limit, the monthly age resolution of ShellChron is sufficient for most typical high-resolution paleoclimate studies.

The ability to produce uninterrupted age models from multi-year records while considering both variability in $\delta^{18}O_w$ and uncertainties on input parameters represent major advantages of ShellChron over previous age modelling solutions. As a result, ShellChron can be applied on a wide range of carbonate archives (see **Fig. 4** and **Table 2**). However, testing ShellChron on different records highlights the limitations of the model inherited through its underlying assumptions. The most accurate model results are obtained on records with minimal growth rate and $\delta^{18}O_w$ variability and a nearly sinusoidal $\delta^{18}O_c$ record, such as tropical **coral** records (**Fig. 4A**; Gagan et al., 1994). In records where large seasonal variability in growth rate and $\delta^{18}O_w$ does occur, such as in intertidal **oyster** shells, ShellChron's accuracy slightly decreases, especially near growth hiatuses in the record (see **Fig. 4B**; Ullmann et al., 2010). A worst-case scenario is represented by the **speleothem** record, which not only suffers from much slower and more unpredictable growth rates but responds to variability in drip water in the cave rather than temperature seasonality, one of the assumptions underlying the current version of ShellChron (**Fig. 4C**; Vansteenberghe et al., 2019). Despite these problems, ShellChron yields an age model that is remarkably accurate on an annual timescale, which is as good as, or better than, the best age model that can be obtained by applying layer counting on the most clearly laminated parts of the speleothem (e.g. Verheyden et al., 2006). It must be noted that, while this is an encouraging result, a major reason for the model's success is the fact that the Proserpine speleothem used in this example is known to receive significantly seasonal (though not sinusoidal) drip water volumes and concentrations

https://doi.org/10.5194/gmd-2020-401
Preprint. Discussion started: 12 February 2021


Geoscientific Model Development Discussions

(Van Rampelbergh, 2014). Variability in drip water properties and cave temperatures are known to differ strongly between cave systems, and ShellChron can therefore only be applied with confidence on speleothem records if consistent seasonal variability in these parameters can be demonstrated (Fairchild et al., 2006; Lachniet, 2009).

The difficulty of applying age model routines on speleothem records highlights one of the main advantages of ShellChron over pre-existing age model routines, namely its modular character. Since $\delta^{18}O_c$ records from some carbonate archives, such as speleothems, cannot be described by the standard combination of temperature and growth rate sinusoids on which ShellChron is based (in its current version), the possibility to adapt the "building block" functions used to approximate these $\delta^{18}O_c$ records (*d18O_model*, *temperature_curve* and *growth_rate_curve*; see **Fig. 1**) while leaving the core structure of ShellChron intact greatly augments the versatility of the model. The freedom to adapt the building blocks used to approximate the $\delta^{18}O_c$ record theoretically enables ShellChron to model sub-annual age-depth relationships in any record as long as the seasonal variability in the variables used to model the input data are predictable and can be represented by a function. For example, since speleothem $\delta^{18}O_c$ records often depend on variability in the $\delta^{18}O_w$ value of the drip water, a function describing this variability through the year can replace the *temperature_curve* function to create more accurate sub-annual age models for speleothems (e.g. Mattey et al., 2008; Lachniet, 2009; Van Rampelbergh et al., 2014). Similarly, the *growth_rate_curve* function can be modified in case the default skewed sinusoid does not accurately describe the extension rate of the record under study, and the *d18O_model* function can be adapted to feature the most fitting $\delta^{18}O_c$-temperature or $\delta^{18}O_c$-$\delta^{18}O_w$ relationship.

By extension, flexibility in the definition of "building block" functions used to approximate the input data paves the way for future application beyond carbonate $\delta^{18}O_c$ records. The seasonal variability in $\delta^{18}O$ in some ice cores can be approximated by a stable and unbiased temperature relationship (van Ommen and Morgan, 1997). ShellChron can therefore be modified to date sub-annual samples in these ice core records and reconstruct seasonal variability in the high latitudes through the Quarternary. Similarly, inter-annual $\delta^{18}O$ variability in tree ring records are demonstrated to record variability in precipitation through the year, and this variability can be modelled to improve sub-annual age models in these records (Xu et al., 2016). More generally, the field of dendrochemistry has recently developed additional chemical

https://doi.org/10.5194/gmd-2020-401
Preprint. Discussion started: 12 February 2021

proxies for seasonality (e.g. trace element concentrations), which can be measured on smaller sample volumes (and thus greater resolution) to obtain ultra-high-resolution records on which (sub-annual) dating can be based (e.g. Poussart et al., 2006; Superville et al., 2017). A similar development has taken place in the study of carbonate bio-archives such as corals and mollusks, of which some show strong, predictable seasonal variability in trace elements (e.g. Mg/Ca and Sr/Ca ratios) which can be used to accurately date these records (de Villiers et al., 1995; Sosdian et al., 2006; Durham et al., 2017). Minor changes in the "building block" functions using empirical transfer functions for these trace element records will enable ShellChron to capitalize on these relationships and reconstruct sub-annual growth rates with improved precision due to the higher precision with which these proxies can be measured compared to $\delta^{18}O_c$ records. Finally, the application of ShellChron for age model construction is not necessarily limited to the seasonal cycle, as other major cycles in climate (e.g. tidal, diurnal or Milankovitch cycles) leave similar marks on climate records and can thus be used as basis for age modelling (e.g. Sano et al., 2012; Huyghe et al., 2019; de Winter et al., 2020a; Sinnesael et al., 2020). It must be noted that, since ShellChron was developed for modeling based on annual periodicity, applying it on other timescales would require more thorough adaptation of the model code than merely adapting the "building block" functions to support additional proxy systems.

While age reconstructions are the main aim of ShellChron, the model also yields information about the temperature and growth rate parameters used in each simulation window to approximate the local $\delta^{18}O_c$ curve. These parameters hold key information about the response of the archive to seasonal changes in the environment, such as the season of growth, relationships between growth rate and temperature and the temperature range that is recorded. By combining these parameters with records of influential environmental variables such as seawater chlorophyl concentration or local precipitation patterns, much can be learned about the climate archive itself and its response to environmental variables, in addition to the climate or environmental change it records. Study examples include the relationship between growth rate of marine calcifies and phytoplankton abundance or the correlation between precipitation patterns and chemical variability in speleothems. While such discussion is beyond the scope of this work, examples of parameter distributions are provided in **SI5**, and the application of modelled growth rate parameters in bivalve sclerochronology is discussed in more detail in Judd et al. (2018). Note that the sliding window approach of ShellChron produces records of changing temperature and growth rate

https://doi.org/10.5194/gmd-2020-401
Preprint. Discussion started: 12 February 2021

parameters at the scale of individual samples (albeit smoothed by the sliding window approach) rather than annually, as in Judd et al. (2018).

6. Conclusions

ShellChron offers a novel, open-source solution to the problem of dating carbonate archives for high-resolution paleoclimate reconstruction on a sub-annual scale. Based on critical evaluation of previous age models, building on their strengths while attempting to eliminate their weaknesses, ShellChron provides continuous age models based on $\delta^{18}O_c$-profiles in these archives with monthly accuracy, taking into account the uncertainties associated with both the model itself and the input data. The monthly accuracy of the model, as tested on a range of virtual and natural datasets, enables its application for age determination in studies of seasonal climate and environmental variability. Higher accuracies can be reached at the cost of longer computation times by adapting the model parameters, but age determinations far beyond the monthly scale are unlikely to be feasible considering the limitations on sampling resolution and measurement uncertainties on $\delta^{18}O_c$ records. ShellChron's computation times on datasets with sampling resolutions typical for the paleoclimatology field (up to 20 samples/yr) remain practical and competitive with previous model solutions, despite adding several features that improve the versatility and interpretation of model results. Its modular design allows ShellChron to be adapted to different situations with comparative ease. It thereby functions as a platform for age-depth modelling on a wide range of climate and environmental archives and is not limited in its application to the $\delta^{18}O_c$ proxy, the carbonate substrate or even to the annual cycle, as long as the relationship between the proxy and the extension rate of the archive on a given time scale can be parameterized. Future improvements will capitalize on this variability, expanding ShellChron beyond its current dependency on the $\delta^{18}O_c$-temperature relationship in carbonates. Members of the high-resolution paleoclimate community are invited to contribute to this effort by adapting the model for their purpose.

Code availability

ShellChron is worked out into a fully functioning package for the open-source computational language R (version 3.5.0 or later; R Core Team, 2020). The most recent full version (v0.2.8) of the ShellChron

https://doi.org/10.5194/gmd-2020-401
Preprint. Discussion started: 12 February 2021


Geoscientific Model Development Discussions

passed the code review of the Comprehensive R Archive Network (CRAN) and is freely available for download as an R package on the CRAN server (see https://CRAN.R-project.org/package=ShellChron). The CRAN server entry also includes detailed line-by-line documentation of the code and working examples for every function. In addition, the development version of ShellChron (currently v0.2.9.9000) is available on GitHub (https://github.com/nielsjdewinter/ShellChron). Those interested in adapting ShellChron for their research purposes are invited to do so here. Code and documentation, together with all supplementary files belonging to this study, are also available on the open-source online repository Zenodo (http://doi.org/10.5281/zenodo.4288344).

Author contribution

NJW designed the study, wrote the model script, carried out the test calculations and wrote the manuscript.

Competing interests

There were no competing interests to declare.

Acknowledgements

This research project is part of the UNBIAS project funded by the European Commission through a Marie Curie Individual Fellowship (MSCA-IF; grant number: 843011) and the Flemish Research Council (FWO; junior postdoc grant, project number: 12ZB220N). Thanks go to Emily Judd for discussions about the workings of the Judd et al. (2018) model and its potential adaptation beyond aragonitic mollusk shells. High-resolution temperature and salinity data from the NIOZ jetty which underlie the **Texel** dataset and the noise added to the idealized **Case 1** dataset were kindly provided by Eric Wagemaakers and Sonja van Leeuwen (Royal Dutch Institute for Sea Research, the Netherlands). The $\delta^{18}O_c$ data series from the *Crassostrea gigas* (**oyster**) and Proserpine stalagmite (**speleothem**) were generously provided by dr. Clemens V. Ullmann (University of Exeter, UK) and dr. Stef Vansteenberge (Vrije Universiteit Brussel, Belgium). Raw data from the *Porites lutea* **coral** dataset were obtained with help of

https://doi.org/10.5194/gmd-2020-401
Preprint. Discussion started: 12 February 2021

Geoscientific Model Development Discussions

610 the WebPlotDigitizer (https://automeris.io/WebPlotDigitizer/) developed by Ankit Rohatgi. Preparation of
611 the ShellChron model into an R package would not have been possible without the helpful instructions
612 by Fong Chun Chan (https://tinyheero.github.io/jekyll/update/2015/07/26/making-your-first-R-
613 package.html), Hilary Parker (https://hilaryparker.com/2014/04/29/writing-an-r-package-from-scratch/)
614 and Hadley Wickham (https://r-pkgs.org/release.html). In addition, distribution of the code in an
615 organized way was made possible thanks to Git (https://git-scm.com/) and Github (https://github.com/)
616 and the R Project Team (https://www.r-project.org/), with special thanks to Uwe Ligges (University of
617 Dortmund, Germany) and Gregor Seyer (University of Vienna, Austria) for their comments on initial
618 submissions of the package to the CRAN database. Thanks go to William A. Huber
619 (https://www.analysisandinference.com/team/william-a-huber-phd) for providing a practical general
620 solution to the peak identification problem in the *cumulative_day* function (see *peakid* function and
621 https://rpubs.com/mengxu/peak_detection).

622

https://doi.org/10.5194/gmd-2020-401
Preprint. Discussion started: 12 February 2021

References

Bajnai, D., Guo, W., Spötl, C., Coplen, T. B., Methner, K., Löffler, N., Krsnik, E., Gischler, E., Hansen, M., Henkel, D., Price, G. D., Raddatz, J., Scholz, D. and Fiebig, J.: Dual clumped isotope thermometry resolves kinetic biases in carbonate formation temperatures, Nature Communications, 11(1), 4005, doi:10.1038/s41467-020-17501-0, 2020.

Baldini, J. U. L., McDermott, F., Hoffmann, D. L., Richards, D. A. and Clipson, N.: Very high-frequency and seasonal cave atmosphere PCO2 variability: Implications for stalagmite growth and oxygen isotope-based paleoclimate records, Earth and Planetary Science Letters, 272(1), 118–129, doi:10.1016/j.epsl.2008.04.031, 2008.

Brand, W. A., Coplen, T. B., Vogl, J., Rosner, M. and Prohaska, T.: Assessment of international reference materials for isotope-ratio analysis (IUPAC Technical Report), Pure and Applied Chemistry, 86(3), 425–467, doi:10.1515/pac-2013-1023, 2014.

de Brauwere, A., De Ridder, F., Pintelon, R., Schoukens, J. and Dehairs, F.: A comparative study of methods to reconstruct a periodic time series from an environmental proxy record, Earth-Science Reviews, 95(3), 97–118, doi:10.1016/j.earscirev.2009.04.002, 2009.

Butler, P. G., Wanamaker, A. D., Scourse, J. D., Richardson, C. A. and Reynolds, D. J.: Variability of marine climate on the North Icelandic Shelf in a 1357-year proxy archive based on growth increments in the bivalve Arctica islandica, Palaeogeography, Palaeoclimatology, Palaeoecology, 373, 141–151, doi:10.1016/j.palaeo.2012.01.016, 2013.

Chauvaud, L., Lorrain, A., Dunbar, R. B., Paulet, Y.-M., Thouzeau, G., Jean, F., Guarini, J.-M. and Mucciarone, D.: Shell of the Great Scallop Pecten maximus as a high-frequency archive of paleoenvironmental changes, Geochemistry, Geophysics, Geosystems, 6(8), doi:10.1029/2004GC000890, 2005.

Coplen, T. B.: Calibration of the calcite–water oxygen-isotope geothermometer at Devils Hole, Nevada, a natural laboratory, Geochimica et Cosmochimica Acta, 71(16), 3948–3957, doi:10.1016/j.gca.2007.05.028, 2007.

Daëron, M., Guo, W., Eiler, J., Genty, D., Blamart, D., Boch, R., Drysdale, R., Maire, R., Wainer, K. and Zanchetta, G.: 13C18O clumping in speleothems: Observations from natural caves and precipitation experiments, Geochimica et Cosmochimica Acta, 75(12), 3303–3317, doi:10.1016/j.gca.2010.10.032, 2011.

Daëron, M., Drysdale, R. N., Peral, M., Huyghe, D., Blamart, D., Coplen, T. B., Lartaud, F. and Zanchetta, G.: Most Earth-surface calcites precipitate out of isotopic equilibrium, Nature Communications, 10(1), 429, doi:10.1038/s41467-019-08336-5, 2019.

De Ridder, F., de Brauwere, A., Pintelon, R., Schoukens, J., Dehairs, F., Baeyens, W. and Wilkinson, B. H.: Comment on: Paleoclimatic inference from stable isotope profiles of accretionary biogenic hardparts—a quantitative approach to the evaluation of incomplete data, by Wilkinson, BH, Ivany, LC, 2002. Palaeogeogr. Palaeocl. Palaeoecol. 185, 95–114, Palaeogeography, Palaeoclimatology, Palaeoecology, 248(3–4), 473–476, 2007.

DeCarlo, T. M. and Cohen, A. L.: Dissepiments, density bands and signatures of thermal stress in Porites skeletons, Coral Reefs, 36(3), 749–761, doi:10.1007/s00338-017-1566-9, 2017.

https://doi.org/10.5194/gmd-2020-401
Preprint. Discussion started: 12 February 2021

663 Dettman, D. L., Reische, A. K. and Lohmann, K. C.: Controls on the stable isotope composition of
664 seasonal growth bands in aragonitic fresh-water bivalves (Unionidae), Geochimica et Cosmochimica
665 Acta, 63(7–8), 1049–1057, 1999.

666 Duan, Q., Sorooshian, S. and Gupta, V.: Effective and efficient global optimization for conceptual
667 rainfall-runoff models, Water resources research, 28(4), 1015–1031, 1992.

668 Dunbar, R. B. and Wellington, G. M.: Stable isotopes in a branching coral monitor seasonal
669 temperature variation, Nature, 293(5832), 453–455, 1981.

670 Durham, S. R., Gillikin, D. P., Goodwin, D. H. and Dietl, G. P.: Rapid determination of oyster lifespans
671 and growth rates using LA-ICP-MS line scans of shell Mg/Ca ratios, Palaeogeography,
672 Palaeoclimatology, Palaeoecology, 2017.

673 Epstein, S., Buchsbaum, R., Lowenstam, H. A. and Urey, H. C.: Revised carbonate-water isotopic
674 temperature scale, Geological Society of America Bulletin, 64(11), 1315–1326, 1953.

675 Fairchild, I. J., Smith, C. L., Baker, A., Fuller, L., Spötl, C., Mattey, D., McDermott, F. and others:
676 Modification and preservation of environmental signals in speleothems, Earth-Science Reviews,
677 75(1), 105–153, 2006.

678 Frisia, S., Borsato, A., Fairchild, I. J. and McDermott, F.: Calcite fabrics, growth mechanisms, and
679 environments of formation in speleothems from the Italian Alps and southwestern Ireland, Journal of
680 Sedimentary Research, 70(5), 1183–1196, 2000.

681 Gagan, M. K., Chivas, A. R. and Isdale, P. J.: High-resolution isotopic records from corals using ocean
682 temperature and mass-spawning chronometers, Earth and Planetary Science Letters, 121(3–4), 549–
683 558, doi:10.1016/0012-821X(94)90090-6, 1994.

684 Goodwin, D. H., Schöne, B. R. and Dettman, D. L.: Resolution and Fidelity of Oxygen Isotopes as
685 Paleotemperature Proxies in Bivalve Mollusk Shells: Models and Observations, PALAIOS, 18(2), 110–
686 125, doi:10.1669/0883-1351(2003)18<110:RAFOOI>2.0.CO;2, 2003.

687 Goodwin, D. H., Paul, P. and Wissink, C. L.: MoGroFunGen: A numerical model for reconstructing
688 intra-annual growth rates of bivalve molluscs, Palaeogeography, Palaeoclimatology, Palaeoecology,
689 276(1), 47–55, doi:10.1016/j.palaeo.2009.02.026, 2009.

690 Grossman, E. L. and Ku, T.-L.: Oxygen and carbon isotope fractionation in biogenic aragonite:
691 temperature effects, Chemical Geology: Isotope Geoscience section, 59, 59–74, 1986.

692 Huybers, P. and Curry, W.: Links between annual, Milankovitch and continuum temperature
693 variability, Nature, 441(7091), 329, 2006.

694 Huyghe, D., de Rafelis, M., Ropert, M., Mouchi, V., Emmanuel, L., Renard, M. and Lartaud, F.: New
695 insights into oyster high-resolution hinge growth patterns, Mar Biol, 166(4), 48, doi:10.1007/s00227-
696 019-3496-2, 2019.

697 IPCC: GLOBAL WARMING OF 1.5 °C an IPCC special report on the impacts of global warming of 1.5 °C
698 above pre-industrial levels and related global greenhouse gas emission pathways, in the context of
699 strengthening the global response to the threat of climate change, sustainable development, and
700 efforts to eradicate poverty. [online] Available from:
701 http://report.ipcc.ch/sr15/pdf/sr15_spm_final.pdf, 2018.

https://doi.org/10.5194/gmd-2020-401
Preprint. Discussion started: 12 February 2021

Ivany, L. C. and Runnegar, B.: Early Permian seasonality from bivalve δ18O and implications for the oxygen isotopic composition of seawater, Geology, 38(11), 1027–1030, 2010.

Jones, D. S.: Sclerochronology: Reading the Record of the Molluscan Shell: Annual growth increments in the shells of bivalve molluscs record marine climatic changes and reveal surprising longevity, American Scientist, 71(4), 384–391, 1983.

Jones, D. S. and Quitmyer, I. R.: Marking Time with Bivalve Shells: Oxygen Isotopes and Season of Annual Increment Formation, PALAIOS, 11(4), 340–346, doi:10.2307/3515244, 1996.

Judd, E. J., Wilkinson, B. H. and Ivany, L. C.: The life and time of clams: Derivation of intra-annual growth rates from high-resolution oxygen isotope profiles, Palaeogeography, Palaeoclimatology, Palaeoecology, 490, 70–83, 2018.

Kim, S.-T. and O'Neil, J. R.: Equilibrium and nonequilibrium oxygen isotope effects in synthetic carbonates, Geochimica et Cosmochimica Acta, 61(16), 3461–3475, doi:10.1016/S0016-7037(97)00169-5, 1997.

Lachniet, M. S.: Climatic and environmental controls on speleothem oxygen-isotope values, Quaternary Science Reviews, 28(5–6), 412–432, 2009.

Le Tissier, M. D. A., Clayton, B., Brown, B. E. and Davis, P. S.: Skeletal correlates of coral density banding and an evaluation of radiography as used in sclerochronology, Marine Ecology Progress Series, 110(1), 29–44, 1994.

LeGrande, A. N. and Schmidt, G. A.: Global gridded data set of the oxygen isotopic composition in seawater, Geophysical research letters, 33(12), 2006.

Lough, J. M.: Climate records from corals, WIREs Climate Change, 1(3), 318–331, doi:10.1002/wcc.39, 2010.

Mahé, K., Bellamy, E., Lartaud, F. and Rafélis, M. de: Calcein and manganese experiments for marking the shell of the common cockle (Cerastoderma edule): tidal rhythm validation of increments formation, Aquat. Living Resour., 23(3), 239–245, doi:10.1051/alr/2010025, 2010.

Mattey, D., Lowry, D., Duffet, J., Fisher, R., Hodge, E. and Frisia, S.: A 53 year seasonally resolved oxygen and carbon isotope record from a modern Gibraltar speleothem: Reconstructed drip water and relationship to local precipitation, Earth and Planetary Science Letters, 269(1), 80–95, doi:10.1016/j.epsl.2008.01.051, 2008.

McCrea, J. M.: On the Isotopic Chemistry of Carbonates and a Paleotemperature Scale, J. Chem. Phys., 18(6), 849–857, doi:10.1063/1.1747785, 1950.

Mitchell Jr., J. M.: An overview of climatic variability and its causal mechanisms, Quaternary Research, 6(4), 481–493, doi:10.1016/0033-5894(76)90021-1, 1976.

Mohr, R. C., Tobin, T. S., Petersen, S. V., Dutton, A. and Oliphant, E.: Subannual stable isotope records reveal climate warming and seasonal anoxia associated with two extinction intervals across the Cretaceous-Paleogene boundary on Seymour Island, Antarctica, Geology, 48(11), 1131–1136, doi:10.1130/G47758.1, 2020.

Müller, P., Taylor, M. H., Klicpera, A., Wu, H. C., Michel, J. and Westphal, H.: Food for thought: Mathematical approaches for the conversion of high-resolution sclerochronological oxygen isotope

https://doi.org/10.5194/gmd-2020-401
Preprint. Discussion started: 12 February 2021

741 records into sub-annually resolved time series, Palaeogeography, Palaeoclimatology, Palaeoecology,
742 440, 763–776, doi:10.1016/j.palaeo.2015.09.032, 2015.

743 O'Donnell, M. S. and Ignizio, D. A.: Bioclimatic predictors for supporting ecological applications in the
744 conterminous United States, US Geological Survey Data Series, 691(10), 2012.

745 Ommen, T. D. van and Morgan, V.: Calibrating the ice core paleothermometer using seasonality,
746 Journal of Geophysical Research: Atmospheres, 102(D8), 9351–9357, doi:10.1029/96JD04014, 1997.

747 Poussart, P. M., Myneni, S. C. B. and Lanzirotti, A.: Tropical dendrochemistry: A novel approach to
748 estimate age and growth from ringless trees, Geophysical Research Letters, 33(17),
749 doi:10.1029/2006GL026929, 2006.

750 R Core Team: R: A Language and Environment for Statistical Computing, R Foundation for Statistical
751 Computing, Vienna, Austria. [online] Available from: https://www.R-project.org/, 2020.

752 Rohling, E. J.: Oxygen isotope composition of seawater, The Encyclopedia of Quaternary Science.
753 Amsterdam: Elsevier, 2, 915–922, 2013.

754 Rollion-Bard, C., Chaussidon, M. and France-Lanord, C.: pH control on oxygen isotopic composition of
755 symbiotic corals, Earth and Planetary Science Letters, 215(1), 275–288, doi:10.1016/S0012-
756 821X(03)00391-1, 2003.

757 Saenger, C., Gabitov, R. I., Farmer, J., Watkins, J. M. and Stone, R.: Linear correlations in bamboo
758 coral δ13C and δ18O sampled by SIMS and micromill: Evaluating paleoceanographic potential and
759 biomineralization mechanisms using δ11B and Δ47 composition, Chemical Geology, 454, 1–14,
760 doi:10.1016/j.chemgeo.2017.02.014, 2017.

761 Sano, Y., Kobayashi, S., Shirai, K., Takahata, N., Matsumoto, K., Watanabe, T., Sowa, K. and Iwai, K.:
762 Past daily light cycle recorded in the strontium/calcium ratios of giant clam shells, Nature
763 Communications, 3, 761, 2012.

764 Schöne, B. R. and Gillikin, D. P.: Unraveling environmental histories from skeletal diaries — Advances
765 in sclerochronology, Palaeogeography, Palaeoclimatology, Palaeoecology, 373, 1–5,
766 doi:10.1016/j.palaeo.2012.11.026, 2013.

767 Schöne, B. R., Fiebig, J., Pfeiffer, M., Gleβ, R., Hickson, J., Johnson, A. L., Dreyer, W. and Oschmann,
768 W.: Climate records from a bivalved Methuselah (Arctica islandica, Mollusca; Iceland),
769 Palaeogeography, Palaeoclimatology, Palaeoecology, 228(1–2), 130–148, 2005.

770 Schöne, B. R., Zhang, Z., Radermacher, P., Thébault, J., Jacob, D. E., Nunn, E. V. and Maurer, A.-F.:
771 Sr/Ca and Mg/Ca ratios of ontogenetically old, long-lived bivalve shells (Arctica islandica) and their
772 function as paleotemperature proxies, Palaeogeography, Palaeoclimatology, Palaeoecology, 302(1–
773 2), 52–64, 2011.

774 Sinnesael, M., De Vleeschouwer, D., Zeeden, C., Batenburg, S. J., Da Silva, A.-C., de Winter, N. J.,
775 Dinarès-Turell, J., Drury, A. J., Gambacorta, G. and Hilgen, F. J.: The Cyclostratigraphy
776 Intercomparison Project (CIP): consistency, merits and pitfalls, Earth-Science Reviews, 102965, 2019.

777 Sosdian, S., Gentry, D. K., Lear, C. H., Grossman, E. L., Hicks, D. and Rosenthal, Y.: Strontium to
778 calcium ratios in the marine gastropod Conus ermineus: Growth rate effects and temperature
779 calibration, Geochemistry, Geophysics, Geosystems, 7(11), 2006.

https://doi.org/10.5194/gmd-2020-401
Preprint. Discussion started: 12 February 2021

780 Steuber, T., Rauch, M., Masse, J.-P., Graaf, J. and Malkoč, M.: Low-latitude seasonality of Cretaceous
781 temperatures in warm and cold episodes, Nature, 437(7063), 1341–1344, 2005.

782 Superville, P.-J., De Winter, N., Phung, A. T., Proix, N., Baeyens, W. and Gao, Y.: Radial metal
783 concentration profiles in trees growing on highly contaminated soils, Chemosphere, 172, 80–88,
784 doi:10.1016/j.chemosphere.2016.12.142, 2017.

785 Tarutani, T., Clayton, R. N. and Mayeda, T. K.: The effect of polymorphism and magnesium
786 substitution on oxygen isotope fractionation between calcium carbonate and water, Geochimica et
787 Cosmochimica Acta, 33(8), 987–996, doi:10.1016/0016-7037(69)90108-2, 1969.

788 Treble, P. C., Schmitt, A. K., Edwards, R. L., McKeegan, K. D., Harrison, T. M., Grove, M., Cheng, H. and
789 Wang, Y. J.: High resolution Secondary Ionisation Mass Spectrometry (SIMS) δ18O analyses of Hulu
790 Cave speleothem at the time of Heinrich Event 1, Chemical Geology, 238(3), 197–212,
791 doi:10.1016/j.chemgeo.2006.11.009, 2007.

792 Uchikawa, J. and Zeebe, R. E.: The effect of carbonic anhydrase on the kinetics and equilibrium of the
793 oxygen isotope exchange in the CO2–H2O system: Implications for δ18O vital effects in biogenic
794 carbonates, Geochimica et Cosmochimica Acta, 95, 15–34, 2012.

795 Ullmann, C. V. and Korte, C.: Diagenetic alteration in low-Mg calcite from macrofossils: a review,
796 Geological Quarterly, 59(1), 3–20, 2015.

797 Ullmann, C. V., Wiechert, U. and Korte, C.: Oxygen isotope fluctuations in a modern North Sea oyster
798 (Crassostrea gigas) compared with annual variations in seawater temperature: Implications for
799 palaeoclimate studies, Chemical Geology, 277(1), 160–166, 2010.

800 Ullmann, C. V., Böhm, F., Rickaby, R. E., Wiechert, U. and Korte, C.: The Giant Pacific Oyster
801 (Crassostrea gigas) as a modern analog for fossil ostreoids: isotopic (Ca, O, C) and elemental (Mg/Ca,
802 Sr/Ca, Mn/Ca) proxies, Geochemistry, Geophysics, Geosystems, 14(10), 4109–4120, 2013.

803 Urban, F. E., Cole, J. E. and Overpeck, J. T.: Influence of mean climate change on climate variability
804 from a 155-year tropical Pacific coral record, Nature, 407(6807), 989–993, doi:10.1038/35039597,
805 2000.

806 Urey, H. C.: Oxygen Isotopes in Nature and in the Laboratory, Science, 108(2810), 489–496, 1948.

807 Van Rampelbergh, M., Verheyden, S., Allan, M., Quinif, Y., Keppens, E. and Claeys, P.: Seasonal
808 variations recorded in cave monitoring results and a 10 year monthly resolved speleothem δ18O and
809 δ13C record from the Han-sur-Lesse cave, Belgium, Climate of the Past Discussions, 10, 1821–1856,
810 2014.

811 Vansteenberge, S., Verheyden, S., Cheng, H., Edwards, R. L., Keppens, E. and Claeys, P.: Paleoclimate
812 in continental northwestern Europe during the Eemian and early Weichselian (125–97 ka): insights
813 from a Belgian speleothem, Clim. Past, 12(7), 1445–1458, doi:10.5194/cp-12-1445-2016, 2016.

814 Vansteenberge, S., Winter, N. de, Sinnesael, M., Verheyden, S., Goderis, S., Malderen, S. J. M. V.,
815 Vanhaecke, F. and Claeys, P.: Reconstructing seasonality through stable isotope and trace element
816 analysis of the Proserpine stalagmite, Han-sur-Lesse Cave, Belgium: indications for climate-driven
817 changes during the last 400 years, Climate of the Past Discussions, 1–32,
818 doi:https://doi.org/10.5194/cp-2019-78, 2019.

819 Verheyden, S., Baele, J.-M., Keppens, E., Genty, D., Cattani, O., Cheng, H., LAWRENCE, E., ZHANG, H.,
820 Van Strijdonck, M. and Quinif, Y.: The Proserpine stalagmite (Han-Sur-Lesse Cave, Belgium):

preliminary environmental interpretation of the last 1000 years as recorded in a layered speleothem, Geologica Belgica, 2006.

de Villiers, S., Nelson, B. K. and Chivas, A. R.: Biological controls on coral Sr/Ca and delta18O reconstructions of sea surface temperatures, Science, 269(5228), 1247, 1995.

Wang, Y. J., Cheng, H., Edwards, R. L., An, Z. S., Wu, J. Y., Shen, C.-C. and Dorale, J. A.: A High-Resolution Absolute-Dated Late Pleistocene Monsoon Record from Hulu Cave, China, Science, 294(5550), 2345–2348, doi:10.1126/science.1064618, 2001.

Watkins, J. M., Hunt, J. D., Ryerson, F. J. and DePaolo, D. J.: The influence of temperature, pH, and growth rate on the δ18O composition of inorganically precipitated calcite, Earth and Planetary Science Letters, 404, 332–343, doi:10.1016/j.epsl.2014.07.036, 2014.

Wilkinson, B. H. and Ivany, L. C.: Paleoclimatic inference from stable isotope profiles of accretionary biogenic hardparts – a quantitative approach to the evaluation of incomplete data, Palaeogeography, Palaeoclimatology, Palaeoecology, 185(1), 95–114, doi:10.1016/S0031-0182(02)00279-1, 2002.

de Winter, N. J., Goderis, S., Dehairs, F., Jagt, J. W., Fraaije, R. H., Van Malderen, S. J., Vanhaecke, F. and Claeys, P.: Tropical seasonality in the late Campanian (late Cretaceous): Comparison between multiproxy records from three bivalve taxa from Oman, Palaeogeography, Palaeoclimatology, Palaeoecology, 485, 740–760, 2017.

de Winter, N., Vellekoop, J., Vorsselmans, R., Golreihan, A., Soete, J., Petersen, S., Meyer, K., Casadio, S., Speijer, R. and Claeys, P.: An assessment of latest Cretaceous Pycnodonte vesicularis (Lamarck, 1806) shells as records for palaeoseasonality: a multi-proxy investigation, Climate of the Past, 14(6), 725–749, 2018.

de Winter, N. J., Goderis, S., Malderen, S. J. M. V., Sinnesael, M., Vansteenberge, S., Snoeck, C., Belza, J., Vanhaecke, F. and Claeys, P.: Subdaily-Scale Chemical Variability in a Torreites Sanchezi Rudist Shell: Implications for Rudist Paleobiology and the Cretaceous Day-Night Cycle, Paleoceanography and Paleoclimatology, 35(2), e2019PA003723, doi:10.1029/2019PA003723, 2020a.

de Winter, N. J., Ullmann, C. V., Sørensen, A. M., Thibault, N., Goderis, S., Van Malderen, S. J. M., Snoeck, C., Goolaerts, S., Vanhaecke, F. and Claeys, P.: Shell chemistry of the boreal Campanian bivalve *Rastellum diluvianum*; (Linnaeus, 1767) reveals temperature seasonality, growth rates and life cycle of an extinct Cretaceous oyster, Biogeosciences, 17(11), 2897–2922, doi:10.5194/bg-17-2897-2020, 2020b.

de Winter, N. J., Vellekoop, J., Clark, A. J., Stassen, P., Speijer, R. P. and Claeys, P.: The giant marine gastropod Campanile giganteum (Lamarck, 1804) as a high-resolution archive of seasonality in the Eocene greenhouse world, Geochemistry, Geophysics, Geosystems, n/a(n/a), e2019GC008794, doi:10.1029/2019GC008794, 2020c.

de Winter, N., Agterhuis, T. and Ziegler, M.: Optimizing sampling strategies in high-resolution paleoclimate records, Climate of the Past Discussions, 1–52, doi:https://doi.org/10.5194/cp-2020-118, 2020d.

Xu, C., Zheng, H., Nakatsuka, T., Sano, M., Li, Z. and Ge, J.: Inter-and intra-annual tree-ring cellulose oxygen isotope variability in response to precipitation in Southeast China, Trees, 30(3), 785–794, 2016.

https://doi.org/10.5194/gmd-2020-401
Preprint. Discussion started: 12 February 2021

Yan, H., Liu, C., An, Z., Yang, W., Yang, Y., Huang, P., Qiu, S., Zhou, P., Zhao, N., Fei, H., Ma, X., Shi, G., Dodson, J., Hao, J., Yu, K., Wei, G., Yang, Y., Jin, Z. and Zhou, W.: Extreme weather events recorded by daily to hourly resolution biogeochemical proxies of marine giant clam shells, PNAS, 117(13), 7038–7043, doi:10.1073/pnas.1916784117, 2020.

Zeebe, R. E.: An expression for the overall oxygen isotope fractionation between the sum of dissolved inorganic carbon and water, Geochemistry, Geophysics, Geosystems, 8(9), doi:10.1029/2007GC001663, 2007.

Zhu, F., Emile-Geay, J., McKay, N. P., Hakim, G. J., Khider, D., Ault, T. R., Steig, E. J., Dee, S. and Kirchner, J. W.: Climate models can correctly simulate the continuum of global-average temperature variability, PNAS, 116(18), 8728–8733, doi:10.1073/pnas.1809959116, 2019.